REMARKS

Claims 1-6 and 9-10 remain pending in the present application. New claim 9 is similar to originally filed claim 6 as amended to include the limitations of originally filed claim 8. Claim 9 is enabling as a power amplifier, and thus overcomes the Examiners 35 U.S.C. §112, second paragraph rejection of original claim 6 in a previous office action. New claim 10 is similar to originally filed claim 7 as amended in accordance with the Examiner's suggestion in a previous office action to form proper antecedent basis. Applicant has attached a marked up version of claims 9-10 to indicate the differences between claims 9-10 and original claims 6-8. The scope of claims 9-10 is at least as broad as original claims 6-8, however, no new matter has been added. All the present claims are believed to be clear and definite and are believed to be patentably distinguished over the prior art of record. Reconsideration of the pending claims and allowance is respectfully requested in view of the following comments.

The 35 U.S.C. §132 objection to the Specification

The Examiner has objected to Applicant's amendment mailed on January 8, 2002 in response to an office action dated September 18, 2001. The objection is pursuant to 35 U.S.C. §132 on the grounds that Applicant's January 8, 2002 amendment introduces new matter. Applicant respectfully disagrees.

As detailed in the VERSION WITH MARKING TO SHOW CHANGES MADE to the Specification that was attached to Applicant's January 8, 2002 amendment, Applicant has simply removed formulas depicted in the figures and added them to the written detailed description of the specification. More specifically, Applicant has removed the characteristic equation from Fig. 1 and added the equation to Paragraph 23 of the specification. Further, Applicant has removed the characteristic null equation depicted on Figs. 2a-2c and added the equation to Paragraph 24 of the detailed description. The proposed drawing corrections removing these equations from Figs. 1 and 2a-2c were approved by the Examiner. For the foregoing reasons,

Applicant respectfully requests the Examiner to remove objections to Applicant's January 8, 2002 amendments to the specification.

The Drawings

Applicant has submitted herewith substitute formal drawings to the Official Draftsperson based on the Examiner's approval.

Claim Rejections pursuant to 35 U.S.C. §112, second paragraph

Claims 4, 5 and 6 were rejected pursuant to 35 U.S.C. §112, second paragraph.

With regard to claim 4, the Examiner has questioned whether the term "multiple feedback filter" as disclosed in claim 4 is well-known in the art. Applicant has attached as Exhibit A Chapter 76 entitled "Single-Amplifier Multiple-Feedback Filters" from <u>The Circuits and Filters Handbook</u>, p. 2372-2384, Wai-Kai Chen ed. (1995). In addition to the title of the chapter, further evidence that the meaning of the term "multiple feedback filter" is well-known in the art is provided by equation 76.7 on page 2373, which is a voltage transfer ratio describing the arrangement commonly referred to as a multiple-loop feedback structure.

The term "state variable filter" as disclosed by claim 5 was similarly questioned by the Examiner with regard to being well-known in the art. Applicant has attached as Exhibit B an excerpt entitled "77.6 State-Variable-Based Biquads" from <u>The Circuits and Filters Handbook</u>, p. 2401-2406, Wai-Kai Chen ed. (1995). As indicated at the bottom of page 2401 and the top of page 2402, filters based on analog computer structures derived from the state-variable representation of linear continuous systems are referred to as state-variable filters. Applicant respectfully requests the removal of the rejection of claims 4 and 5 pursuant to 35 U.S.C. §112, second paragraph since claims 4 and 5 particularly point out and distinctly claim the subject matter of the invention, and are therefore proper.

Claim 6 has been amended as the Examiner has recommended as detailed in the attached version with markings to show changes made. Accordingly, Applicant respectfully requests the removal of the rejection pursuant to 35 U.S.C. §112, second paragraph of claim 6.

Claim Rejections pursuant to 35 U.S.C. §102(b)

Claims 1, 4 and 5 were rejected pursuant to 35 U.S.C. §102(b) as being anticipated by Chew et al. (U.S. Patent No. 5,107,491 hereinafter referred to as "Chew"). Applicant respectfully disagrees for at least the following reasons.

Applicant's Claim 1 discloses an active low-pass filter system that includes a low-pass filter circuit and an isolated-integrator band-reject filter. The low-pass filter circuit includes a resistive forward signal flow branch. The isolated-integrator band-reject filter is coupled with the low pass circuit forward signal flow branch.

Chew teaches, in Fig. 1, a single low pass filter stage 12 and a notch filter stage 14 (band reject filter). The output 40 of the low pass filter stage 12 is coupled to the input 42 of the notch filter stage 14. In contradistinction to Chew, claim 1 discloses that the isolated-integrator band-reject filter is coupled with the resistive forward signal flow branch of the low pass filter circuit. Referring to Figs. 2a-2c and 4, it is clearly illustrated that coupling of the isolated-integrator band-reject filters (20) with the resistive forward signal flow branch(es) does not occur at the output (Out) of the low pass filter circuit (22, 24, 26, 28, 30). (see specification paragraphs 24, 26, 28 and 44) Accordingly, the isolated-integrator band-reject filter is not coupled with an output of the low pass filter circuit as taught by Chew, and Chew does not suggest or disclose the configuration disclosed by claim 1. In fact, Chew does not teach a resistive forward signal flow branch in a low pass filter circuit at all. Accordingly, Applicant respectfully requests the Examiner to withdraw the rejections pursuant to 35 U.S.C. §102(b) of claim 1 and corresponding dependent claims 4 and 5 which depend therefrom.

Claim Rejecti ns pursuant to 35 U.S.C. §103(a)

Claim 2 was rejected pursuant to 35 U.S.C. §103(a) as being anticipated by Chew in view of prior art Fig. 1 of Applicant's specification. Claim 3 was rejected pursuant to 35 U.S.C. §103(a) as being anticipated by Chew in view of Sallen et al. Applicant respectfully traverses these rejections for at least the following reasons.

Chew has been discussed previously. The Examiner has postulated that it would have been obvious for one skilled in the art to use the prior art Fig. 1 isolated-integrator band-reject filter for the notch filter of Chew. As previously discussed, Chew fails to teach, suggest or disclose that the isolated-integrator band-reject filter is coupled with the resistive forward signal flow branch of a low-pass filter circuit. As such, including a resistor for tuning within the low-pass filter circuit as disclosed by claim 2 is clearly not obvious. Following the teaching of Chew and prior art Fig. 1 provides the resistor for tuning beyond the output of a low pass filter not within the low pass filter as disclosed by claims 1 and 2. Similarly, coupling the isolated-integrator band-reject filter with the resistive forward signal flow branch of Sallen & Key filter is clearly not obvious. The combined teaching of Chew and Sallen et al. at best provides a notch filter coupled to the <u>output</u> of a Sallen & Key filter, not an isolated-integrator band-reject filter within a Sallen & Key filter as disclosed by claims 1 and 3. Accordingly, for at least the foregoing reasons, Applicant respectfully requests the removal of the 35 U.S.C. §103(a) rejection of claims 2 and 3.

Applicant believes that claims 1-6 and 9-10 are allowable in their present form and that this application is in condition for allowance. Accordingly, it is respectfully requested that the Examiner so find and issue a Notice of Allowance in due course. Should the Examiner deem a telephone conference to be beneficial in expediting allowance of this application, the Examiner is invited to call the undersigned attorney at the telephone number listed below. No fees are

believed to be due at this time, however, should any fees be deemed required, please charge such fees therefor to Deposit Account No. 23-1925.

Respectfully submitted,

Sanders N. Hillis
Attorney Reg. No. 45,712

Attachments: VERSION WITH MARKINGS TO SHOW CHANGES MADE pgs. 8-9.
Exhibits A and B

BRINKS HOFER GILSON & LIONE
One Indiana Square, Suite 2425
Indianapolis, Indiana 46204-2033
Telephone: (317) 636-0886
Fax: (317) 634-6701

VERSION WITH MARKINGS TO SHOW CHANGES MADE

Please amend Claim 6 and add Claims 9-10 as follows:

6. (Twice Amended) A power amplifier system for driving a load comprising:

a pulse width modulation power circuit creating ripple spectra;

an error amplifier and modulator circuit connected to an input of the pulse width modulation circuit;

a demodulation filter connected between said pulse width modulation power circuit and the load;

a feedback control loop coupled to said error amplifier and modulator [pulse width modulation power] circuit and including:

an active low-pass filter;

a first resistive voltage divider circuit coupled between the output of said demodulation filter and a first input of said low-pass filter;

a feedback demodulation filter coupled to a second input of said low-pass filter and including at least one isolated-integrator band-reject filter; and

a second resistive voltage divider circuit coupled between the output of said pulse width modulation power circuit and said feedback demodulation filter.

Load connect resistor

[6.]9. (New) A power amplifier system for driving a load comprising:

a pulse width modulation circuit having an input and an output, said pulse width modulation circuit operable to creat[ing]e ripple spectra;

an error amplifier and modulator circuit connected to said input of said pulse width modulation circuit;

a demodulation filter connected to said output of said pulse width modulation circuit;

a feedback control loop coupled to said error amplifier and modulator circuit and to said output of said pulse width modulation circuit, said feedback control loop [and] including [an active low-pass filter, said low-pass filter including] a feedback demodulation filter, [and] wherein an isolated-integrator frequency-rejecting network is included as part of said feedback demodulation filter.

[7.]10. (New) The system of Claim [6]9, wherein [the] said isolated-integrator frequency-rejecting network is an isolated-integrator band-reject filter, including a resistor for tuning the band-reject filter.

EXHIBIT "A"

CHAPTER 7.6

ENTITLED

"SINGLE-AMPLIFIER MULTIPLE-FEEDBACK FILTERS"

PGS. 2372-2384 (9 pgs.)

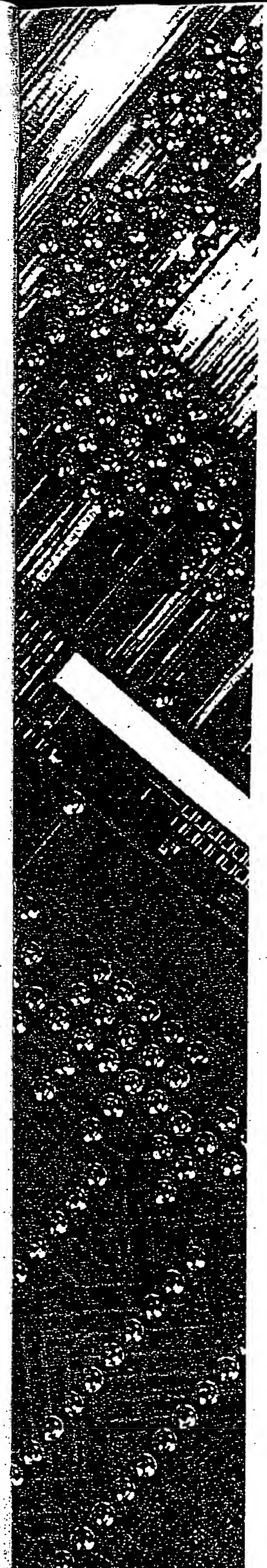

THE CIRCUITS and FILTERS HANDBOOK

Editor-in-Chief

WAI-KAI CHEN
University of Illinois
Chicago, Illinois

CRC PRESS   IEEE PRESS

A CRC Handbook Published in Cooperation with IEEE Press

Library of Congress Cataloging-in-Publication Data

The circuits and filters handbook / editor-in-chief, Wai-Kai Chen.
p. cm. -- (The electrical engineering handbook series)
Includes bibliographical references and index.
ISBN 0-8493-8341-2 (acid-free paper)
1. Electronic circuits. 2. Electric filters. I. Chen, Wai-Kai.
1936– II. Series.
TK7867.C4977 1995
621.3815 -- dc20

95-7037
CIP

International Standard Book Number 0-8493-8341-2
Library of Congress Card Number 95-7037
Printed in the United States of America 1 2 3 4 5 6 7 8 9 0
Printed on acid-free paper

76

Single-Amplifier Multiple-Feedback Filters

F. William Stephenson
Virginia Polytechnic Institute and State University

76.1 Introduction

In this section we will consider the design of second-order sections that incorporate a single operational amplifier. Such designs are based upon one of the earliest approaches to *RC* active filter synthesis, which has proven to be a fundamentally sound technique for over 30 years. Furthermore, this basic topology has formed the basis for designs as technology has evolved from discrete component assemblies to monolithic realizations. Hence, the circuits presented here truly represent reliable well-tested building blocks for sections of modest selectivity.

76.2 General Structure for Single-Amplifier Filters

The general structure of Fig. 76.1 forms the basis for the development of infinite-gain single-amplifier configurations. Simple circuit analysis may be invoked to obtain the open-circuit voltage transfer function. For the passive network:

$$I_1 = y_{11}V_1 + y_{12}V_2 + y_{13}V_3 \tag{76.1}$$

$$I_2 = y_{21}V_1 + y_{22}V_2 + y_{23}V_3 \tag{76.2}$$

$$I_3 = y_{31}V_1 + y_{32}V_2 + y_{33}V_3 \tag{76.3}$$

For the amplifier, ideal except for finite gain A:

$$V_3 = -AV_2 \tag{76.4}$$

0-8493-8341-2/95/$0.00+$.50

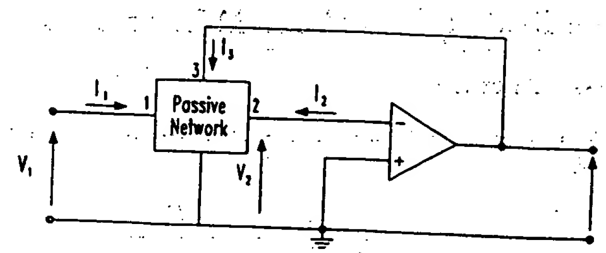

FIGURE 76.1 General infinite-gain single-amplifier structure.

Noting that $I_2 = 0$, the above equations reduce to the following expression for the voltage transfer function:

$$\frac{V_3}{V_1} = \frac{-y_{31}}{y_{32} + \dfrac{y_{33}}{A}} \tag{76.5}$$

As $A \to \infty$, which we can expect at low frequencies, the above expression reduces to the more familiar

$$\frac{V_3}{V_1} = -\frac{y_{31}}{y_{32}} \tag{76.6}$$

Theoretically, a wide range of transfer characteristics can be realized by appropriate synthesis of the passive network [1]. However, it is not advisable to extend synthesis beyond second-order functions for structures containing only one operational amplifier due to the ensuing problems of sensitivity and tuning. Furthermore, notch functions require double-element replacements [2] or parallel ladder arrangements [3], which are nontrivial to design, and whose performance is inferior to that resulting from other topologies such as those discussed in Chapters 77 and 78.

While formal synthesis techniques could be used to meet particular requirements, the most common approach is to use a double-ladder realization of the passive network, as shown in Fig. 76.2. This arrangement, commonly referred to as the multiple-loop feedback (MFB) structure, is described by the following voltage transfer ratio:

$$\frac{V_3}{V_1} = \frac{-Y_1 Y_3}{Y_5(Y_1 + Y_2 + Y_3 + Y_4) + Y_3 Y_4} \tag{76.7}$$

This negative feedback arrangement yields highly stable realizations. The basic all-pole (low-pass, bandpass, high-pass) functions can be realized by single-element replacements for the admittances $Y_1, \cdots, Y_5$, as described in the following subsection.

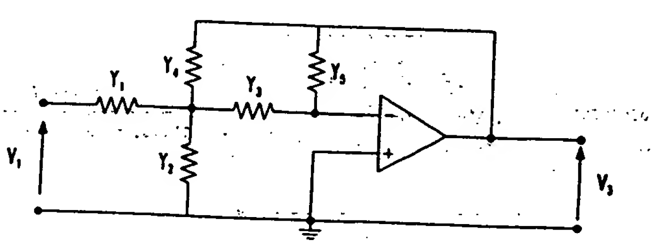

FIGURE 76.2 General double ladder multiple-feedback network.

76.3 All-Pole Realizations of the MFB Structure

Low-Pass Structure

The general form of the second-order all-pole low-pass structure is described by the following transfer ratio:

$$\frac{V_3}{V_1} = \frac{H}{s^2 + \frac{\omega_p s}{Q_p} + \omega_p^2} \tag{76.8}$$

By comparing the above requirement with (76.7) it is clear that both Y_1 *and* Y_3 must represent conductances. Furthermore, by reviewing the requirements for the denominator, Y_5 *and* Y_2 must be capacitors, while Y_4 is a conductance.

High-Pass Structure

The general form of the second-order all-pole high-pass transfer function is

$$\frac{V_3}{V_1} = \frac{Hs^2}{s^2 + \frac{\omega_p s}{Q_p} + \omega_p^2} \tag{76.9}$$

TABLE 76.1 MFB All-Pole Realizations

Filter Type	Network	Voltage Transfer Function
Lowpass	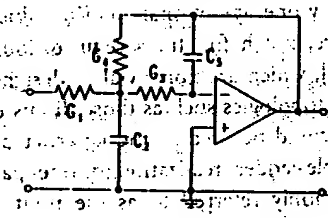	$\dfrac{-G_1G_3}{s^2C_2C_5 + sC_5(G_1+G_3+G_4) + G_3G_4}$
Highpass	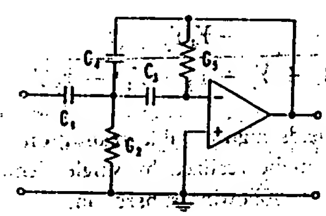	$\dfrac{-s^2C_1C_3}{s^2C_3C_4 + sG_5(C_1+C_3+C_4) + G_2G_5}$
Bandpass	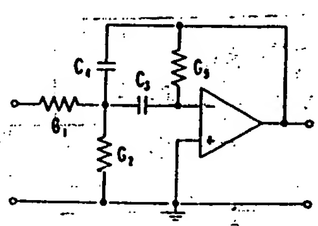	$\dfrac{-sG_1C_3}{s^2C_3C_4 + sG_5(C_3+C_4) + G_5(G_1+G_2)}$

With reference to Eq. (76.7), it is seen that both Y_1 *and* Y_3 must represent capacitors. There is a need for a third capacitor ($Y_4 = sC_4$) to yield the s^2 term in the denominator function. The remaining two elements Y_2 *and* Y_5, represent conductances.

Bandpass Structure

The general form of the second-order all-pole bandpass transfer function is

$$\frac{V_3}{V_1} = \frac{Hs}{s^2 + \frac{\omega_p s}{Q_p} + \omega_p^2} \tag{76.10}$$

Two solutions exist since Y_1 *and* Y_3 can be either capacitive or conductive. Choosing $Y_1 = G_1$ and $Y_3 = sC_3$ yields $Y_4 = sC_4$ and Y_2, Y_5 are both conductances.

The general forms of the above realizations are summarized in Table 76.1 [4].

76.4 MFB All-Pole Designs

MFB designs are typically reserved for sections having a pole-Q of 10 or less. One of the reasons for this constraint is the reliance upon component ratios for achieving Q. This can be illustrated by consideration of the low-pass structure for which

$$\frac{V_3}{V_1} = \frac{-G_1G_3}{s^2C_2C_5 + sC_5(G_1 + G_3 + G_4) + G_3G_4} \tag{76.11}$$

By comparison with (76.8),

$$Q_p = \frac{\sqrt{C_2C_5G_3G_4}}{C_5(G_1 + G_3 + G_4)}$$

or, in terms of component ratios:

$$Q_p = \frac{\sqrt{C_2}}{\sqrt{C_5}}\left\{\frac{1}{\frac{G_1}{\sqrt{G_3G_4}} + \sqrt{\frac{G_3}{G_4}} + \sqrt{\frac{G_4}{G_3}}}\right\} \tag{76.12}$$

Hence, high Q_p can only be achieved by means of high component spreads. In general terms, a Q_p of value n requires a component spread proportional to n^2.

Filter design is effected by means of coefficient matching. Thus, for the low-pass case, comparison of like coefficients in (76.8) and the transfer ratio in Table 76.1 yields

$$G_1G_3 = H \tag{76.13}$$

$$C_2C_5 = 1 \tag{76.14}$$

$$C_5(G_1 + G_3 + G_4) = \frac{\omega_p}{Q_p} \tag{76.15}$$

$$G_3G_4 = \omega_p^2 \tag{76.16}$$

These equations do not yield an equal-capacitor solution but can be solved for equal-resistor pairs. Hence, if $G_1 = G_3$,

$$G_1 = G_3 = \sqrt{H} \qquad \text{[from (76.13)]}$$

$$G_4 = \frac{\omega_p^2}{\sqrt{H}} \qquad \text{[from (76.16)]}$$

Then,

$$C_5 = \frac{\omega_p \sqrt{H}}{Q_p(2H + \omega_p^2)} = \frac{1}{C_2}$$

An alternative solution for which $G_3 = G_4$ is shown in Table 76.2, together with equal-capacitor designs for the bandpass and high-pass cases.

The conditions [4] for maximum Q_p in the bandpass realization require $C_3 = C_4$ and $G_1 = G_2 = nG_5$, where n is a real number. This yields a maximum Q_R of $\sqrt{n/2}$, and requires that $H = \omega_p Q_p$.

TABLE 76.2 Element Values for the MFB All-Pole Realizations

Element (Table 76.1)	Low-Pass	Bandpass	High-Pass
Y_1	$G_1 = \frac{H}{\omega_p}$	$G_1 = H$	$C_1 = H$
Y_2	$C_2 = \frac{Q_p(2\omega_p^2 + H)}{\omega_p^2}$	$G_2 = 2\omega_p Q_p - H$	$G_2 = \omega_p(2+H)Q_p$
Y_3	$G_3 = \omega_p$	$C_3 = 1$	$C_3 = 1$
Y_4	$G_4 = G_3$	$C_4 = C_3$	$C_4 = C_3$
Y_5	$C_5 = \frac{\omega_p^2}{Q_p(2\omega_p^2 + H)}$	$G_5 = \frac{\omega_p}{2Q_p}$	$G_5 = \frac{\omega_p}{Q_p(2+H)}$

Example 1. Using the cascade approach, design a four-pole Butterworth bandpass filter having a Q of 5, a center frequency of (1.5) kHz, and midband gain of 20 dB. Assume that only 6800 pF capacitors are available.

Solution. The lowpass prototype is the second-order Butterworth characteristic having a dc gain of 10 (i.e., 20 dB). Thus,

$$T(s) = \frac{10}{s^2 + \sqrt{2}s + 1} \qquad \text{(i)}$$

The low-pass-to-bandpass frequency transformation for a Q of 5 entails replacing s in (i) by $5(s + 1/s)$. This yields the following bandpass function for realization:

$$\frac{V_o}{V_i} = \frac{0.4s^2}{s^4 + 0.28284s^3 + 2.04s^2 + 0.28284s + 1}$$

$$= \underbrace{\frac{-sH_1}{(s^2 + .15142s + 1.15218)}}_{\text{(section 1)}} \cdot \underbrace{\frac{-sH_2}{(s^2 + .13142s + .86792)}}_{\text{(section 2)}} \qquad \text{(ii)}$$

$$Q_1 = Q_2 = 7.089$$
$$\omega_{p1} = 1.0734 \qquad \omega_{p2} = 0.9316$$

As expected, the Q-factors of the cascaded sections are equal in the transformed bandpass characteristic. However, the order of cascade is still important. So as to reduce the noise output of the filter, it is necessary to apportion most of the gain to section 1 of the cascade. Section 2 then filters out the noise without introducing excessive passband gain. In the calculation that follows, it is important to note that the peak gain of a bandpass section is given by HQ/ω_p.

Since the overall peak gain of the cascade is to be 10, let this also be the peak gain of section 1. Hence,

$$\frac{H_1 Q_1}{\omega_{p1}} = 6.6041 H_1 = 10$$

giving $H_1 = 1.514$.

Furthermore, from (ii):

$$H_1 H_2 = 0.4$$

so that $H_2 = 0.264$.

The design of each bandpass section proceeds by coefficient matching, conveniently simplified by Table 76.2. Setting $C_3 = C_4 = 1$ F, the normalized resistor values for section 1 may be determined as

$$R_1 = 0.661\ \Omega; \qquad R_2 = 0.073\ \Omega; \qquad R_5 = 13.208\ \Omega$$

The impedance denormalization factor is determined as

$$z_n = \frac{10^{12}}{2\pi \times 1500 \times 6800} = 15{,}603$$

Thus, the final component values for section 1 are

$$C_1 = C_2 = 6800 \text{ pF}$$
$$\left.\begin{aligned} R_1 &= 10.2 \text{ k}\Omega \\ R_2 &= 1.13 \text{ k}\Omega \\ R_5 &= 205 \text{ k}\Omega \end{aligned}\right\} \text{ Standard 1 percent values}$$

Note the large spread in resistance values ($R_5/R_2 \simeq 4Q^2$) and the fact that this circuit is only suitable for low-Q realizations. It should also be noted that the amplifier open-loop gain at ω_p must be much greater than $4Q^2$ if it is not to cause significant differences between the design and measured values of Q.

The component values for section 2 are determined in an identical fashion.

Example 2. Design the MFB bandpass filter characterized in Example 1 as a high-pass/low-pass cascade of second-order sections. Use the design equations of Table 76.2 and, where possible, set capacitors equal to 5600 pF. It is suggested that you use the same impedance denormalization factor in each stage. Select the nearest preferred 1 percent resistor values.

Solution. Since the peak gain of the overall cascade is to be 10, let this also be the gain of stage 1 (this solution yields the best noise performance). The peak gain of the low-pass section is given by

$$\frac{H_1 Q}{\sqrt{1 - 1/2Q^2}} = 7.16 H_1 = 10 \qquad \therefore \underline{\underline{H_1 = 1.397}}$$

The overall transfer function (from Example 1) is

$$\frac{V_o}{V_i} = \frac{0.4s^2}{s^4 + 0.2824s^3 + 2.04s^2 + 0.2824s + 1}$$

$$\therefore H_1 H_2 = 0.4 \quad \text{so that} \quad \underline{\underline{H_2 = 0.286}}$$

Thus, assuming a low-pass/high-pass cascade, we have

$$\underbrace{\frac{1.397}{s^2 + 0.15145 + 1.1522}}_{\text{section 1}} \cdot \underbrace{\frac{0.286s^2}{s^2 + 0.1314s + 0.8679}}_{\text{section 2}}$$

Design the low-pass section (section 1) using Table 76.2 to yield

$$G_1 = \frac{H_1}{\sqrt{1.15218}} = 1.301, \quad \text{so that} \quad R_1 = 0.7684\ \Omega$$

$$C_2 = \frac{(2\omega_p^2 + H_1)}{\omega_p^2} Q_p = 22.77\ \text{F}$$

$$G_3 = \omega_p = 1.0733, \quad \text{so that} \quad R_3 = 0.9316\ \Omega = R_4$$

$$C_5 = 1/C_2 = 0.0439\ \text{F}$$

Now, design the high-pass section (section 2):

$$C_1' = 0.286\ \text{F}$$

$$G_2' = \omega_p(2 + H_2)Q = 15.099, \quad \text{so that} \quad R_2' = 0.0662\ \Omega$$

$$C_3' = C_4' = 1\ \text{F}$$

$$G_5' = \frac{\omega_p}{Q_p(2 + H)} = 0.0574, \quad \text{so that} \quad R_5' = 17.397\ \Omega$$

To obtain as many 5600 pF capacitors as possible, the two sections should be denormalized separately. However, in this example, a single impedance denormalization will be used. Setting $C_3' = C_4' = 5600$ pF yields $z_n = 18\,947$.

This leads to the following component values:

Low-pass stage	High-pass stage
$R_1 = 2.204$ kΩ (2.21 kΩ)	$C_1' = 1602$ pF
$C_2 = 0.128$ μF	$R_2' = 1.254$ kΩ (1.24 kΩ)
$R_3 = 17.651$ kΩ (17.8 kΩ) $= R_4$	$C_3' = C_4' = 5600$ pF
$C_5 = 246$ pF	$R_5' = 329.62$ kΩ (332 kΩ)

1 percent values in parentheses.

76.5 Practical Considerations in the Design of MFB Filters

Sensitivity, the effects of finite amplifier gain, and tuning are all of importance in practical designs. The following discussion is based upon the bandpass case.

Sensitivity

Taking account of finite amplifier gain A, but assuming $R_{in} = \infty$ and $R_o = 0$ for the amplifier, the bandpass transfer function becomes

$$\frac{V_3}{V_1} = \frac{-sG_1/C_4\left(1+\frac{1}{A}\right)}{s^2 + s\left\{\frac{G_5(C_3+C_4)}{C_3C_4} + \frac{G_1+G_2}{C_4(1+A)}\right\} + \left\{\frac{G_5(G_1+G_2)}{C_3C_4}\right\}} \tag{76.17}$$

which is identical to the expression in Table 76.1 if $A = \infty$.

Assuming a maximum Q design,

$$Q = \frac{Q_p}{1 + \frac{2Q_p^2}{(1+A)}} \tag{76.18}$$

where Q_p is the desired selectivity and Q is the actual Q-factor in the presence of finite amplifier gain.

If $A \gg 2Q - 1$, the classical Q-sensitivity may be derived as

$$S_A^Q = \frac{2Q^2}{A} \tag{76.19}$$

which is uncomfortably high. By contrast, the passive sensitivities are relatively low:

$$S_{C_3,C_4}^Q = 0 \qquad S_{G_5}^Q = -0.5 \qquad S_{G_1,G_2}^Q = 0.25$$

while the ω_p sensitivities are all ± 0.5.

Effect of Finite Amplifier Gain

The effect of finite amplifier gain can be further illustrated by plotting (76.18) for various Q-factors, and for two commercial operational amplifiers. Assuming a single-pole roll-off model, the frequency dependence of open-loop gain for $\mu A741$ and $LF351$ amplifiers is as follows.

Frequency (Hz)	Gain	
	μA741	LF351
10	1.3×10^5	3.16×10^5
100	10^4	3.16×10^4
1000	10^3	3.16×10^3
10 000	10^2	3.16×10^2

Figure 76.3 shows the rather dramatic fall-off in actual Q as frequency increases (and hence gain decreases). Thus, for designs of modest Q (note that $A \gg 2Q - 1$), a very high quality amplifier is needed if the center frequency is more than a few kilohertz. For example, the LF351 with a unity gain frequency of 4 MHz will yield 6 percent error in Q at a frequency of only 1 kHz.

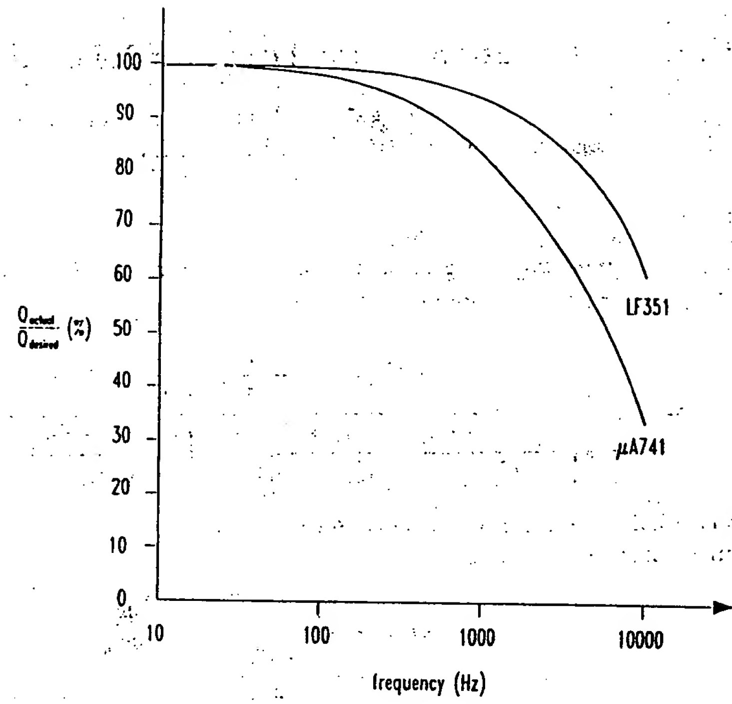

FIGURE 76.3 Effect of finite amplifier gain on the design Q for MFB bandpass realizations using two commercial operational amplifiers.

Tuning

Limited functional tuning of the bandpass section is possible. For example, the midband (peak) gain

$$K_o = \frac{G_1 C_3}{G_5(C_3 + G_4)} \tag{76.20}$$

may be adjusted by means of either G_1 or G_5.

Subsequent adjustment of either Q_p or ω_p is possible via G_2. In view of the discussion above, it is most likely that adjustment of Q_p will be desired. However, since the expressions for Q_p and ω_p are so similar, any adjustment of Q_p is likely to require an iterative procedure to ensure that ω_p does not change undesirably.

A more desirable functional tuning result is obtained in circumstances in which it is necessary to preserve a constant bandwidth, i.e., in a spectrum analyzer. Since

$$\omega_p = \sqrt{G_5(G_1 + G_2)/C_3 C_4} \tag{76.21}$$

and

$$B = \frac{\omega_p}{Q_p} = G_5(C_3 + C_4) \tag{76.22}$$

adjustment of G_2 will allow for a frequency sweep without affecting K_o or B.

An alternative to functional tuning may be found by adopting deterministic [5] or automatic [6] tuning procedures. These are particularly applicable to hybrid microelectronic or monolithic realizations.

76.6 Modified Multiple-Loop Feedback (MMFB) Structure

In negative feedback topologies such as the MFB, "high" values of Q_p are obtained at the expense of large spreads in element values. By contrast, in positive feedback topologies such as those attributed to Sallen and Key, Q_p is enhanced by subtracting a term from the s^1 (damping) coefficient in the denominator. The two techniques are combined in the MMFB (Deliyannis) arrangement [7] of Fig. 76.4.

Analysis of the circuit yields the bandpass transfer function given by

$$\frac{V_o}{V_i} = \frac{-sC_3G_1(1+k)}{s^2C_3C_4 + s\{G_5(C_3+C_4) - kC_3G_1\} + G_1G_5} \tag{76.23}$$

where $k = G_b/G_a$, and the Q-enhancement term "$-kC_3G_1$" signifies the presence of positive feedback. This latter term is also evident in the expression for Q_p:

$$Q_p = \frac{\sqrt{G_1/G_5}}{\left\{\sqrt{\dfrac{C_4}{C_3}} + \sqrt{\dfrac{C_3}{C_4}} - k\dfrac{G_1}{G_5}\sqrt{\dfrac{C_1}{C_2}}\right\}} \tag{76.24}$$

The design process consists of matching coefficients in (76.23) with those of the standard bandpass expression of (76.10). The design steps have been conveniently summarized by Huelsman [8] for the equal-capacitor solution and the following procedure is essentially the same as that described by him.

Example 3. Design a second-order bandpass filter with a center frequency of 1 kHz, a pole-Q of 8, and a maximum resistance spread of 50. Assume that the only available capacitors are of value 6800 pF.

1. The above constraint suggests an equal-valued capacitor solution. Thus, set $C_3 = C_4 = C$.
2. Determine the resistance ratio parameter n_o that would be required if there were no positive feedback. From Section 76.4, $n_o = 4Q_p^2 = 256$.

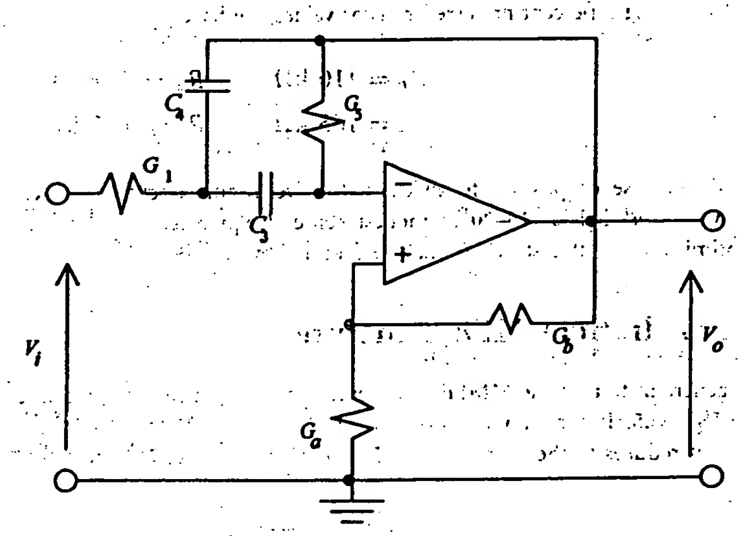

FIGURE 76.4 Modified multiple-loop feedback (MMFB) structure.

3. Select the desired ratio n (where n is greater than 1 but less than 256) and use it to determine the amount of positive feedback k. From (76.24),

$$Q_p = \frac{\sqrt{n}}{2 - kn}$$

so that

$$k = \frac{1}{\sqrt{n}}\left\{\frac{2}{\sqrt{n}} - \frac{1}{Q_p}\right\}$$

Since $n = 50$ and $Q_p = 8$, $k = 0.0316$.

4. A convenient value may now be selected for R_B. If $R_B = 110$ kΩ, then $R_A = R_B\ (0.0316) = 3.48$ kΩ.
5. Since, from (76.23),

$$\omega_p = \sqrt{\frac{G_1 G_5}{C_3 C_4}}$$

and $G_1/G_5 = n$ we may determine G_5 as

$$G_5 = \frac{\omega_p C}{\sqrt{n}}$$

Since $C = 6800$ pF, $n = 50$, and $G_5 = 1/R_5$:

$$R_5 = \frac{\sqrt{50}}{2\pi 10^3 \times 6.8 \times 10^{-9}} = 165.5\ \text{k}\Omega$$

Hence $R_1 = R_5/n = 3.31$ kΩ.

6. Using 1 percent preferred resistor values, we have

$$R_B = 110\ \text{k}\Omega \qquad R_A = 3.16\ \text{k}\Omega$$
$$R_5 = 165\ \text{k}\Omega \qquad R_1 = 3.48\ \text{k}\Omega$$

Judicious use of positive feedback in the Deliyannis circuit can yield bandpass filters with Q values as high as 15–20 at modest center frequencies. A more detailed discussion of the optimization of this structure may be found elsewhere [9].

76.7 Biquadratic MMFB Structure

A generalization of the MMFB arrangement, yielding a fully biquadratic transfer ratio is shown in Fig. 76.5. If the gain functions K_1, K_2, K_3 are realized by resistive potential dividers, the circuit reduces to the more familiar Friend biquad of Fig. 76.6, for which

$$\frac{V_o}{V_i} = \frac{cs^2 + ds + e}{s^2 + as + b} \qquad (76.25)$$

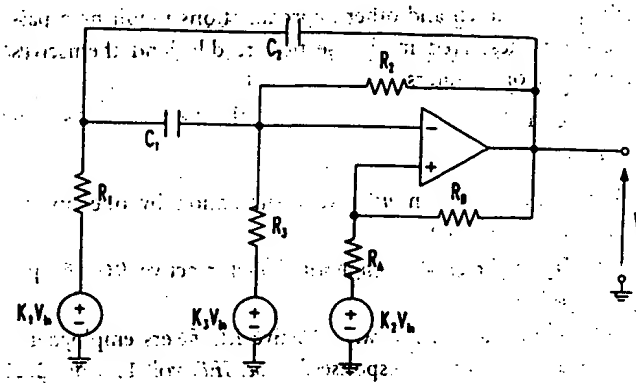

FIGURE 76.5 A generalization of the MMFB circuit.

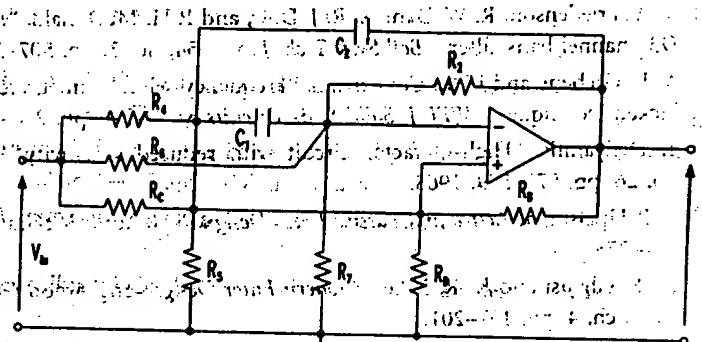

FIGURE 76.6 The Friend biquad.

where

$$K_1 = \frac{R_5}{R_4 + R_5}; \quad K_2 = \frac{R_D}{R_c + R_D}; \quad K_3 = \frac{R_7}{R_6 + R_7}$$
$$R_1 = \frac{R_4 R_5}{R_4 + R_5}; \quad R_A = \frac{R_c R_D}{R_c + R_D}; \quad R_3 = \frac{R_6 R_7}{R_6 + R_7} \qquad (76.26)$$

This structure is capable of yielding a full range of biquads of modest pole Q, including notch functions derived as elliptic characteristics of low modular angle. It was used extensively in the Bell System, where the benefits of large-scale manufacture were possible. Using the standard tantalum thin film process, and deterministic tuning by means of laser trimming, quite exacting realizations were possible [10]. The structure is less suited to discrete component realizations. Although design is possible by coefficient matching, the reader is referred to an excellent step-by-step procedure developed by Huelsman [11].

76.8 Conclusions

The multiple-feedback structure is one of the most basic active filter building blocks. It is extremely reliable when used to realize low-Q (< 10), low frequency (up to 15 kHz) second-order sections of the low-pass, bandpass, and high-pass forms. Stability is ensured by the negative feedback topology, though component spreads are proportional to Q^2.

The disadvantage of larger component spread may be reduced by the judicious use of positive feedback. This approach may be extended to yield the widely used Friend biquad, which allows the realization of notch and other approximations requiring a pair of imaginary zeros.

All networks described in this section readily lend themselves to the cascade method for realizing higher-order filters.

References

[1] G. K. Aggarwal, "On nth order simulation by one operational amplifier," *Proc. IEEE*, vol. 52, p. 969, 1969.

[2] P. L. Taylor, "Flexible design method for active *RC* two-ports," *Proc. IEE*, vol. 110, pp. 1607–1616, 1963.

[3] A. G. J. Holt and J. I. Sewell, "Active *RC* filters employing a single operational amplifier to obtain biquadratic responses," *Proc. IEE*, vol. 112, pp. 2227–2234, 1965.

[4] P. Bowron and F. W. Stephenson, *Active Filters for Communications and Instrumentation*, Berkshire, England: McGraw-Hill, 1979, p. 170.

[5] R. A. Friedenson, R. W. Daniels, R. J. Dow, and P. H. McDonald, "*RC* active filters for the *D*3 channel bank filter," *Bell Syst. Tech. J.*, vol. 54, no. 3, pp. 507–529, 1975.

[6] A. B. Grebene and H. R. Camenzind, "Frequency-selective integrated circuits using phase-locked techniques," *IEEE J. Solid-State Circuits*, vol. SC-4, pp. 216–225, Aug. 1969.

[7] T. Deliyannis, "High-*Q* factor circuit with reduced sensitivity," *Electron. Lett.*, vol. 4, no. 26, pp. 577–579, 1968.

[8] L. P. Huelsman, *Active and Passive Filter Design*, New York: McGraw-Hill, 1993, ch. 5, pp. 277–278.

[9] M. S. Ghausi and K. R. Laker, *Modern Filter Design*, Englewood Cliffs, NJ: Prentice Hall, 1981, ch. 4, pp. 197–201.

[10] J. J. Friend, C. A. Harris, and D. Hilberman, "STAR: An active biquadratic filter section," *IEEE Trans. Circuits Syst.*, vol. CAS-22, pp. 115–121, Feb. 1975.

[11] L. P. Huelsman, "Multiple-loop feedback filters," in *RC Active Filter Design Handbook* (F. W. Stephenson, Ed.), New York: Wiley, 1985, ch. 7, pp. 201–203.

EXHIBIT "B"

SECTION 77.6

ENTITLED

"STATE-VARIABLE-BASED BIQUADS"

PGS. 2401-2406 (5 pgs.)

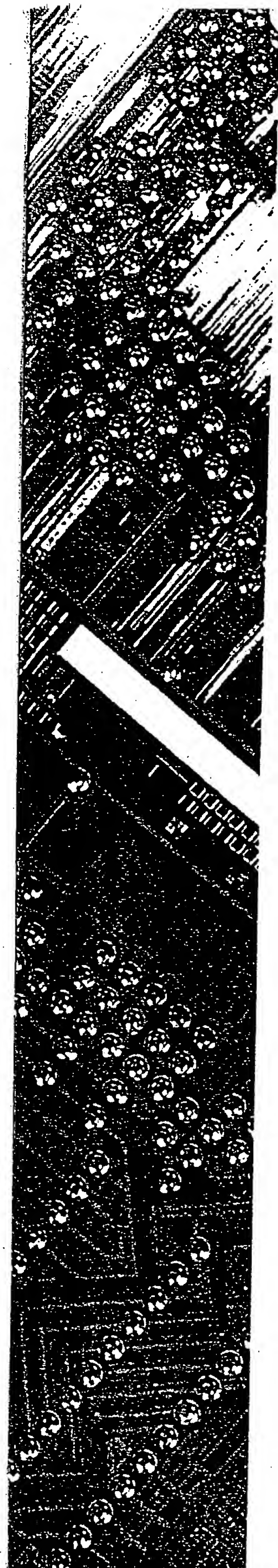

THE CIRCUITS and FILTERS HANDBOOK

Editor-in-Chief

WAI-KAI CHEN
University of Illinois
Chicago, Illinois

CRC PRESS IEEE PRESS

A CRC Handbook Published in Cooperation with IEEE Press

Library of Congress Cataloging-in-Publication Data

The circuits and filters handbook / editor-in-chief, Wai-Kai Chen.
p. cm. -- (The electrical engineering handbook series)
Includes bibliographical references and index.
ISBN 0-8493-8341-2 (acid-free paper)
1. Electronic circuits. 2. Electric filters. I. Chen, Wai-Kai.
1936- II. Series.
TK7867.C4977 1995
621.3815 -- dc20

95-7037
CIP

International Standard Book Number 0-8493-8341-2
Library of Congress Card Number 95-7037
Printed in the United States of America 1 2 3 4 5 6 7 8 9 0
Printed on acid-free paper

derived from the state-variable representation of linear continuous systems. Therefore, these filters are also referred to as *state-variable filters.*

Figure 77.25(a) shows the basic analog computer structure consisting of one summing amplifier and two integrators. We assume both integrators to have the same transfer function $-1/(sT)$, where T is called the integrator time constant. Analyzing this structure yields

$$V_1 = -K_1 \cdot V_3 + K_2 \cdot V_i + K_3 \cdot V_2 \tag{77.65}$$

$$V_2 = -\frac{1}{sT} \cdot V_1 \tag{77.66}$$

$$V_3 = -\frac{1}{sT} \cdot V_2 \tag{77.67}$$

which results in

$$H_{HP}(s) = \frac{V_1}{V_i} = \frac{s^2T^2K_2}{s^2T^2 + sTK_3 + K_1} \tag{77.68}$$

Using (77.66), we can immediately derive the voltage transfer ratio V_2/V_i from (77.68):

$$H_{BP}(s) = \frac{V_2}{V_i} = \frac{-sTK_2}{s^2T^2 + sTK_3 + K_1} \tag{77.69}$$

Finally, with (77.67) we obtain from (77.69)

$$H_{LP}(s) = \frac{V_3}{V_i} = \frac{K_2}{s^2T^2 + sTK_3 + K_1} \tag{77.70}$$

Thus, the structure in Fig. 77.25(a) simultaneously realizes a high-pass filter, a bandpass filter, and a low-pass filter. The corresponding filter circuit, proposed by Kerwin, Huelsman, and Newcomb is depicted in Fig. 77.25(b). The integrators consist of one op-amp, one resistor R, and one capacitor C. The time constant is given by $T = RC$. The three gain factors of the

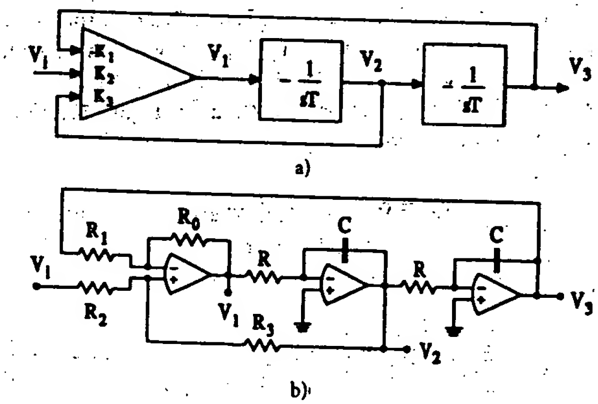

FIGURE 77.25 (a) Second-order analog computer structure and (b) state-variable filter section proposed by Kerwin, Huelsman, and Newcomb.

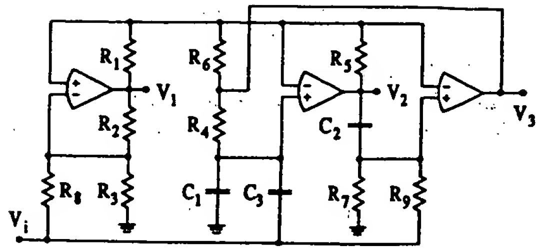

FIGURE 77.24 Padukone–Mulawka–Ghausi biquad.

with

$$N_3(s) = s^2C_1C_2G_1G_9 + sC_2(G_7G_8G_3 + G_8G_2G_3 - G_8G_1G_4) + (G_9G_7G_{10}G_5 + G_9G_{10}G_2G_5 - G_9G_{10}G_4G_6) \quad (77.60)$$

and

$$D(s) = s^2C_1C_2(G_1G_9 + G_2G_9) + sC_2(G_7G_8G_3 + G_7G_8G_4) + (G_9G_7G_{10}G_5 + G_9G_{10}G_7G_6) \quad (77.61)$$

The two other output nodes lead to similar transfer expressions.

The second biquad, which is based on the resonator in Fig. 77.22, was proposed by Padukone, Mulawka, and Ghausi [11] and is depicted in Fig. 77.24. Assuming ideal op-amps and choosing V_3 as output voltage, we obtain the following transfer function:

$$H_3(s) = \frac{V_3}{V_i} = \frac{N_3(s)}{D(s)} \quad (77.62)$$

with

$$N_3(s) = s^2[C_2C_3(G_2G_6 - G_1G_3) + C_1C_2G_1G_8] + s[C_1G_2G_5G_9 - C_3G_2G_5G_7 + C_2G_1G_4G_8] + (G_2G_4G_5G_9) \quad (77.63)$$

and

$$D(s) = s^2(C_1 + C_3)C_2G_2G_6 + sC_2G_1G_4(G_3 + G_8) + G_2G_4G_5(G_7 + G_9) \quad (77.64)$$

It has been shown [11] that the pole sensitivities to all passive components are not greater than unity. The filter section has the main advantage of being particularly insensitive to gain–bandwidth variations even when the op-amps are mismatched.

77.6 State-Variable-Based Biquads

A frequency used multiple-amplifier biquad is the circuit proposed by Kerwin, Huelsman and Newcomb [8]. This filter circuit has extreme flexibility, good performance, and low sensitivities to the passive components. The filter is based on analog computer structures [13], which are

summing amplifier are determined by the four resistors R_0–R_3:

$$K_1 = \frac{R_0}{R_1} \tag{77.71}$$

$$K_2 = \frac{R_3}{R_2 + R_3}\left(1 + \frac{R_0}{R_1}\right) \tag{77.72}$$

$$K_3 = \frac{R_2}{R_2 + R_3}\left(1 + \frac{R_0}{R_1}\right) \tag{77.73}$$

Obviously, the integrator time constant T plays the role of a reciprocal normalization frequency. Thus, if we refer the frequency variable s to $1/T$, we obtain from (77.70) the normalized low-pass transfer function:

$$H_{LP}(s) = \frac{V_3}{V_i} = \frac{K_2}{s^2 + sK_3 + K_1} \tag{77.74}$$

Given the normalized pole frequency ω_p and the pole Q-factor Q_p, we can design the filter section by equating

$$K_1 = \omega_p^2 \tag{77.75}$$

and

$$K_3 = \omega_p/Q_p \tag{77.76}$$

Then K_2 is fixed by the dc gain of the transfer function:

$$K_2 = H_0 \tag{77.77}$$

The state-variable filter circuit can be extended to a general biquad by adding an output amplifier that sums the three voltages V_1, V_2, and V_3. Figure 77.26(a) shows a state-variable filter with an output amplifier summing the voltages V_1, V_2, and V_3 of the circuit in Fig. 77.25(b). This biquad has been proposed also by Kerwin, Huelsman and Newcomb [8]. As alternative circuits, the amplifiers in Fig. 77.26(b) and (c) can be used. Figure 77.26(b) shows an output amplifier that realizes the following sum:

$$V_o = \alpha_1 V_1 + \alpha_2 V_2 + \alpha_3 V_3 \tag{77.78}$$

with

$$\alpha_1 = -\frac{R_{10}}{R_{11}} \qquad \alpha_2 = \frac{R_{14}}{R_{12} + R_{14}}\left(1 + \frac{R_{10}}{R_{11}\|R_{13}}\right) \qquad \alpha_3 = -\frac{R_{10}}{R_{13}} \tag{77.79}$$

If we solve (77.68)–(77.70) for the three output voltages and substitute them in (77.79) with normalized variables s we obtain

$$H(s) = \frac{V_o}{V_i} = -K_2\frac{|\alpha_1|s^2 + |\alpha_2|s + |\alpha_3|}{D(s)} \tag{77.80}$$

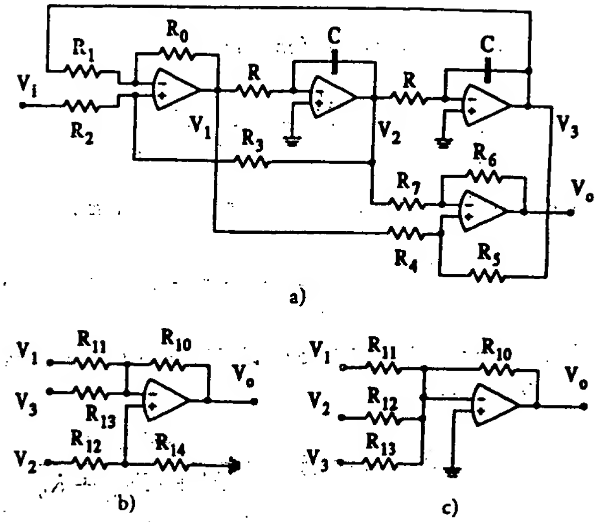

FIGURE 77.26 (a) State-variable filter with output amplifier, (b) output amplifier with inverting and noninverting inputs, and (c) output amplifier with three inverting inputs.

All numerator coefficients have the same sign. Therefore, the zeros of the transfer function are in the left-s-half plane. If we set $\alpha_2 = 0$, i.e., if we delete the voltage divider R_{12}, R_{14} and ground the noninverting input terminal of the op-amp, we obtain zeros on the $j\omega$ axis.

When designing the biquad, R_{14} and R_{10} may be used to scale the impedance level of the two resistive subnetworks. Then from the three numerator coefficients or from the overall gain constant of the transfer function, the zero frequency ω_z and the zero Q-factor Q_z we can easily determine the remaining resistors R_{11}, R_{12}, and R_{13}.

The output amplifier in Fig. 77.26(c) has three inverting inputs. Summing the voltages V_1, V_2, and V_3 leads to a numerator polynomial where the sign of the middle coefficient is different from the sign of the other two. Thus, the zeros are in the right-s-half plane. Again, we can delete the resistor R_{12} to realize zeros on the $j\omega$ axis.

A second state-variable biquad circuit proposed by Tow and Thomas [3], [16], [17] yields similar performance to that of the Kerwin–Huelsman–Newcomb circuit. It uses a feedback loop with one damped integrator, one integrator, and one inverting amplifier; see Fig. 77.27(a). Figure 77.27(b) shows the Tow–Thomas circuit with three op-amps.

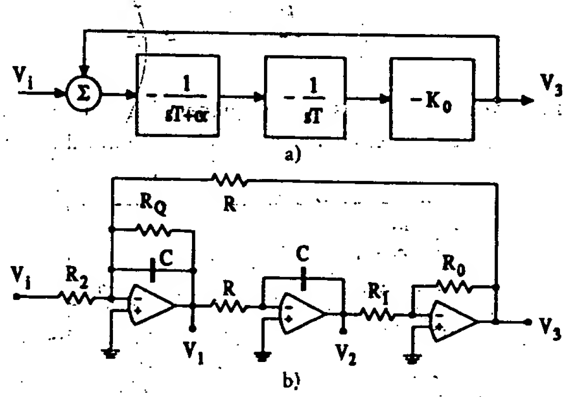

FIGURE 77.27 (a) Principle and (b) three-op-amp realization of the Tow–Thomas filter.

The damped integrator has a transfer function

$$\frac{V_1}{V_3} = \frac{-1}{sT + \alpha}\bigg|_{V_i=0} \tag{77.81}$$

with $T = RC$ and $\alpha = R/R_Q$. The inverting amplifier has a gain

$$\frac{V_3}{V_2} = -\frac{R_0}{R_1} = -K_0 \tag{77.82}$$

An analysis of the circuit in Fig. 77.27(b) with V_i being the input voltage and V_3 the output voltage yields a transfer function

$$H_{LP}(s) = \frac{V_3}{V_i} = \frac{-K_0\alpha_2}{s^2T^2 + sTK_Q + K_0} \tag{77.83}$$

with

$$K_0 = \frac{R_0}{R_1} \qquad \alpha_2 = \frac{R}{R_2} \qquad K_Q = \frac{R}{R_Q} \tag{77.84}$$

For the design of the filter, the integrator time constant T serves as a reciprocal normalization frequency. Then, from the predefined normalized pole frequency we can determine the resistor ratio K_0, from the pole Q-factor the ratio K_Q, and from the dc gain of the filter section the ratio α_i. Choosing convenient values for C and R_0, we finally determine the resistors R, R_1, R_Q, and R_2 from the parameters T, K_0, K_Q, and α_2, respectively.

The filter circuit in Fig. 77.26 requires an additional op-amp to realize a transfer function with a general second-degree numerator polynomial. An alternative method is to feed fractions of the input signal forward into the input of each op-amp. This is realized in the multiple-input Tow–Thomas biquad [3]; see Fig. 77.28. The transfer function of this circuit can be calculated to be

$$H(s) = \frac{V_o}{V_i} = -\frac{s^2T^2\alpha_4 + sT[K_Q\alpha_4 - K_0\alpha_3] + [K_0(\alpha_2 - K_Q\alpha_3)]}{s^2T^2 + sTK_Q + K_0} \tag{77.85}$$

with K_0, α_2, and K_Q as defined in (77.84) and

$$\alpha_3 = \frac{R}{R_3} \qquad \alpha_4 = \frac{R_0}{R_4} \tag{77.86}$$

Thus, arbitrary numerator coefficients can be predescribed. In particular, if we choose $\alpha_3 = \alpha_4 = 0$ we obtain the low-pass filter circuit in Fig. 77.27(b) and the transfer function in (77.83).

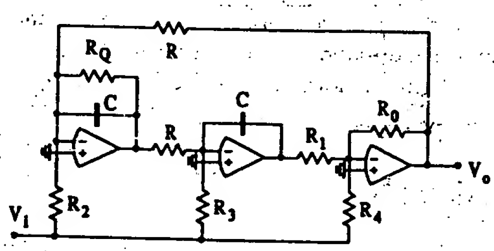

FIGURE 77.28 Generalized Tow–Thomas biquad.

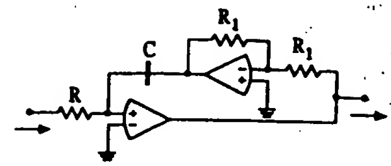

FIGURE 77.29 Noninverting integrator using an additional op-amp to compensate for phase lag.

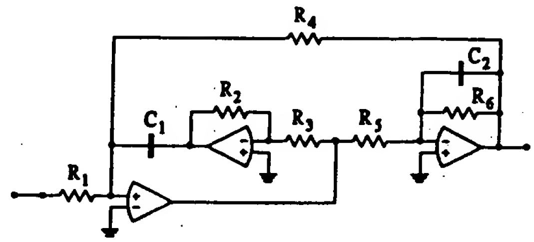

FIGURE 77.30 Åkerberg–Mossberg biquad.

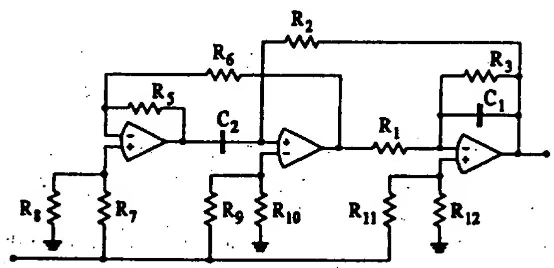

FIGURE 77.31 Berka–Herpy biquad.

When the state-variable filters described above are used to realize high-Q filter functions, the Q practically obtained is usually higher than that desired in the design. This effect is called Q enhancement and is caused by the phase lag introduced by the nonideal op-amps. One way to solve this problem is to use integrators with phase compensation.

Figure 77.29 shows a noninverting integrator with an additional op-amp for phase lag compensation. A detailed description of this circuit can be found in [7]. Putting this noninverting integrator together with an inverting integrator in a feedback loop results in a resonator with a Q-factor that is almost independent of the gain–bandwidth product of the op amps. Thus, nearly no Q enhancement occurs.

Exactly this feedback loop is used in the Åkerberg–Mossberg biquad [1]; see Fig. 77.30. In this circuit, a noninverting integrator with phase lag compensation together with an inverting damped integrator is connected as a feedback loop. More details about this filter section can be found in [1], [6], [7].

Finally, let us consider the general biquad proposed by Berka and Herpy [2]; see Fig. 77.31. This biquad is also based on a state-variable representation and requires a second-order differentiator and a damped integrator. One of the main advantages of this circuit are the extremely low sensitivities. A detailed description of the filter circuit and its design can be found in [6].

77.7 All-Pass-Based Biquads

Finally, we will briefly consider two circuits that are based on first-order all-pass sections. Figure 77.32 shows the classical filter circuit introduced by Tarmy and Ghausi [15].